

Amine Hamdi<sup>1,2</sup>, Sidi Mohammed Merghache<sup>2</sup>, Toufik Aliouane<sup>1</sup>

## Effect of cutting variables on bearing area curve parameters (BAC-P) during hard turning process

Hard turning is a machining process that is widely used in the precision mechanical industry. The characterization of the functional surface texture by the ISO 13565 standard holds a key role in automotive mechanics. Until now, the impact of cutting conditions during hard turning operation on the bearing area curve parameters has not been studied (ISO 13565). The three parameters  $R_{pk}$ ,  $R_k$  and  $R_{vk}$  illustrate the ability of the surface texture to resist friction. In this work, the main objective is to study the impact of cutting conditions ( $V_c$ ,  $f$  and  $ap$ ) of the hard turning on three parameters of the bearing area curve. The statistical study based on response surface methodology (RSM), analysis of variance (ANOVA) and quadratic regression were performed to model the three output parameters and optimize the input parameters. The experimental design used in this study is the Taguchi  $L_{25}$  orthogonal array. The results obtained show that the cutting speed has a greater effect on the bearing ratio curve ( $R_{pk}$ ,  $R_k$  and  $R_{vk}$ ) parameters with a percentage contribution of 37.68%, 37.65% and 36.91%, respectively. The second significant parameter is the feed rate and the other parameter is significant only in relation to  $R_{pk}$  and  $R_k$  parameters.

### 1. Introduction

The machining and finishing processes of functional surfaces by material removal are very numerous, among which one can mention turning, milling, grinding, hard turning, belt grinding, etc. Hard turning has proven to be an interesting process in dry machining. It contributes significantly to reducing the total cost of machining precision parts.

---

✉ Amine Hamdi, e-mail: [hamdi\\_amine@ymail.com](mailto:hamdi_amine@ymail.com)

<sup>1</sup>Laboratory of Applied Optics (LAO), Institute of Optics and Precision Mechanics, University Ferhat Abbas Setif 1, 19000, Algeria.

<sup>2</sup>Institute of Sciences & Technology, University Center of Tissemsilt, 38000, Algeria.



© 2020. The Author(s). This is an open-access article distributed under the terms of the Creative Commons Attribution-NonCommercial-NoDerivatives License (CC BY-NC-ND 4.0, <https://creativecommons.org/licenses/by-nc-nd/4.0/>), which permits use, distribution, and reproduction in any medium, provided that the Article is properly cited, the use is non-commercial, and no modifications or adaptations are made.

Hard turning process (HTP) is defined as a turning operation of hard metals (steel and cast iron) [1]. These materials are treated and thermally hardened, with hardness in the range 45–65 HRC [2] or between 45 and 70 HRC [3]. The tools used in this case have specific properties such as wear resistance, temperature resistance, good chemical stability, etc. Ceramics and cubic boron nitride (CBN) have rendered possible industrial use of this technology. The development of this process was motivated by the need to find an alternative to costly traditional grinding processes. The latter is often long, costly, not flexible and damaging to the environment. Its environmental hazard is due to the coolants used during the machining of precision mechanical parts [4, 5]. Hard turning offers the advantages of reduced costs, reduced production time, improved product quality and achieve close tolerances in terms of surface finish [6]. Hard turning of steel parts with a hardness greater than 60 HRC with mixed ceramic cutting tools and PCBN is one of the most interesting processes for precise finishing [7, 8]. Currently, this process is desirable instead of grinding, in order to increase productivity [9]. During manufacturing process by hard turning, a white layer at surface layer of the machined part appears. The layer formed during hard machining is generally a hard and brittle phase, what exactly is a problem in the commissioning phase. According to Duan et al. [10], the relationship between the white layer thickness and feed rate, carbon content and hardness of material is proportional. According to Revel et al. [11], the AISI 52100 bearing steel turning of medium hardness (61 HRC) using CBN cutting insert improves surface integrity. Therefore, the roughness average  $Ra$  of 0.1 to 0.2  $\mu\text{m}$  is within the limits obtained by grinding. In addition, this process produces a white layer  $< 1 \mu\text{m}$  on the machined part surface and induces compressive residual stresses.

Until now, many studies were conducted on surface texture, material removal rate, cutting tool wear, cutting efforts, cutting power and cutting tool vibration, related to hard turning operations. Saini et al. [12] used response surface methodology (RSM) and the BOX-Behnken design of experiments to predict surface roughness and tool wear. The experimental data were obtained through 29 turning tests of hardened AISI H-11 steel (48–50 HRC). The data show that good surface quality can be obtained with low feed rate and high cutting speed. However, the drawback of a high cutting speed is a higher wear of the cutting tool. In this respect, Manivel and Gandhinathan [13] studied via the Taguchi method  $L_{18}$  orthogonal array, optimization and interactions of cutting parameters on surface roughness ( $Ra$ ) and tool wear ( $Vb$ ). The machined material is austempered ductile iron (grade 3), hardness 45 HRC and tensile strength 1241 MPa. A CVD coated carbide cutting tool was used. The ANOVA analysis indicates that the cutting speed has a contribution of 49.1% and 50.2%, respectively. They found that cutting speed is the most influential parameter on both input parameters ( $Ra$  and  $Vb$ ). Bartarya and Choudhury [14] reported that depth of cut is the first factor affecting the three cutting forces ( $F_x$ ,  $F_y$  and  $F_z$ ) when turning EN31 steel ( $60 \pm 2$  HRC) using uncoated CBN tool. The second factor is the feed rate and the last is the cutting speed. The study was based

on experimental and numerical results of hard turning cold work tool steel AISI D3 (60 HRC) using a ceramic cutting tool and a complete factorial plan  $3^3$  (27 trials).

Aouici et al. [15] investigated the impact of three machining parameters of dry hard turning ( $V_c$ ,  $f$  and  $ap$ ) and the workpiece hardness ( $H$ ) by machining hot work steel AISI H11. Three different levels of workpiece hardness (40, 45 and 50 HRC) and CBN cutting tool, commercially known as CBN7020 (the standard designation is SNGA12 04 08 S01020) were used. After a statistical analysis by ANOVA and mathematical modeling by RSM of four output parameters ( $R_a$ ,  $F_x$ ,  $F_y$  and  $F_z$ ), the results show that the workpiece hardness and the depth of cut ( $H$  and  $ap$ ) are primarily influenced by the three components of the cutting force. Furthermore, workpiece hardness and feed rate have particular influence on the surface roughness. According to Azizi et al. [16], the three machining parameters most affecting arithmetic average roughness ( $R_a$ ) during hard turning of AISI 52100 bearing steel by coated  $Al_2O_3 + TiC$  mixed ceramic cutting tool are: feed rate ( $f$ ), workpiece hardness ( $H$ ) and cutting speed ( $V_c$ ). Moreover, the depth of cut ( $ap$ ), the workpiece hardness ( $H$ ) and feed rate ( $f$ ) are the most influential parameters on the three cutting force components. Shihab et al. [17] presented a micro-channel development in the insert to supply the cutting fluid directly at the tool-chip interface. This new design has been shown to reduce the flank wear by 48.87% during dry hard turning and 3.04% during wet hard turning. The authors found that this tool saves about 87.5% in the consumption of volume of cutting fluid and energy.

In his works, Jouini et al. [18, 19] examined the relationship between rolling contact fatigue life (RCFL) and surface quality. Precision hard turning (PHT) tests using CBN cutting tool were made on AISI 52100 hardened bearing steel rings with an average hardness of  $61 \pm 1$  HRC. The conclusion drawn from these practical studies highlights a relationship between the RCFL and the roughness amplitude  $R_a$ . The RCFL reaches 5.2 million cycles for  $R_a = 0.11 \mu m$ , 1.2 million cycles for  $R_a = 0.2 \mu m$  and 0.32 million cycles for  $R_a = 0.25 \mu m$ . Therefore, the RCF life of the ground bearing components reaches 3.2 million cycles for  $R_a = 0.05 \mu m$ . Furthermore, the surface roughness of precision hard turning is of the order of 0.1 to 0.2  $\mu m$ . The grinding process produces values close to or less than the precision hard turning values. In general, the precision hard turning process (PHTP) improves the surface integrity of functional surfaces (surface texture, residual stresses and white layer) [20]. Rotella et al. [21] did a comparative study in 2012 between dry and cryogenic hard turning. The material and cutting inserts used are hardened steel (AISI 52100) and cubic boron nitride (CBN). After a series of experiments under different conditions of cutting speed and feed rate, the researchers in question indicate that cryogenic cooling improves surface integrity, product life and functional performance.

Meddour et al. [22] studied the impact of cutting parameters and the nose radius of mixed ceramic tool on both output parameters: the arithmetic mean roughness ( $R_a$ ) and the three force components ( $F_x$ ,  $F_y$  and  $F_z$ ). Hard turning experiences are made on AISI 52100 bearing steel (59 HRC) and through a central composite

design (CCD) of 30 tests. The results of the statistical analysis (ANOVA) and graphic (RSM) in question researchers have shown that the depth of cut is the first machining parameter influencing the three force components, followed by the feed rate. Moreover, the nose radius affects only the thrust force ( $F_y$ ). However, the feed rate and nose radius are two parameters with significant influence on surface roughness. More recently, Meddour et al. [23] modeled the surface roughness ( $R_a$ ) and the three cutting force components when turning AISI 4140 hardened steel (60 HRC). The cutting tool used in the experimental part was of mixed ceramic (70%  $Al_2O_3$  and 30% TiC). The modeling was performed through three approaches. The first is quadratic regression by the response surface method. The others are the artificial neural networks (ANN) and the non-dominated sorting genetic algorithm (NSGA-II). The output responses are better predicted by the ANN technique than by quadratic regression. On the other hand, the results of optimization by NSGA-II are more efficient than those of the desirability function method (DF), which uses second-order RSM models. In addition, the tool nose radius was shown to affect the surface roughness more than the technological parameters during hard turning of AISI 52100 steel (60 HRC) by coated CBN tool [24].

The present study aims at statically analyzing the impact of hard machining parameters (cutting speed ( $V_c$ ), feed rate ( $f$ ) and depth of cut ( $ap$ )) and their interactions on the parameters of material ratio curve ( $R_{pk}$ ,  $R_k$  and  $R_{vk}$ ) and finding the role of each machining parameter. This analysis employs RSM, ANOVA and the quadratic regression to model the output parameters. The purpose of this study is to minimize  $R_{pk}$  and  $R_k$  parameters while maximizing  $R_{vk}$  parameter to improve the quality of bearing area curve (BAC).

## 2. Experimental procedures

### 2.1. Workpiece material, cutting insert and tool holder

The studied material is a 16MC5 casehardened steel (%C 0.14/0.18), subjected to induction hardening and quenched in oil at a temperature of 860°C, followed by income to 200°C. Its surface hardness after income was 52 HRC. The chemical composition is given in Table 1. This steel is recommended especially for the manufacture of parts subjected to high efforts such as camshafts, gears, etc.

Table 1.

Chemical composition of 16MC5 steel

% by mass	% C	% Mn	% Cr	% Si	% S
Measured value	0.16	1.22	0.63	0.06	0.01

The samples of 30 mm diameter were machined using a conventional lathe with 6.6 KW power and a ceramic tool having good edge retention, strong toughness

and high wear resistance. Its designation according to the ISO standard is: SNGN 12 08 08 (see Fig. 1) while that of the tool holder used is: CSSNR3225 P12.

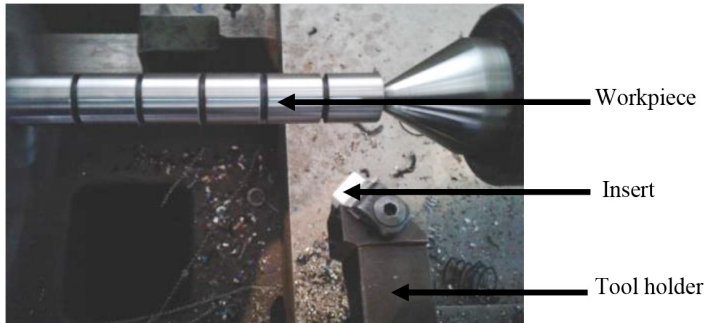


Fig. 1. Work-tool setup in lathe

## 2.2. Measurements of the parameters of bearing area curve

The parameters measurements of the bearing ratio curve were made on a 2D Taylor Hobson profilometer with a diamond stylus radius of  $2\ \mu\text{m}$  (Precision Measurement System Form Talysurf 120), using a Gaussian filter and a cut-off wavelength set to  $0.8\ \text{mm}$ . The roughness profiles were measured over an evaluation length equal to  $L_n = 4.8\ \text{mm}$ , according to ISO 13565 standard. Each surface was characterized by three measurements in different locations and the average value is used in the study.

The measured parameters of the material ratio curve (MRC) during all hard turning tests are:  $R_{pk}$  – reduced peak height,  $R_k$  – core roughness depth,  $R_{vk}$  – reduced valley depth (ISO 13565 standard). The functional parameters  $R_{pk}$ ,  $R_k$  and  $R_{vk}$  are determined from the Abbott-Firestone curve “bearing area curve: bearing ratio curve: material ratio curve” (see Fig. 2).

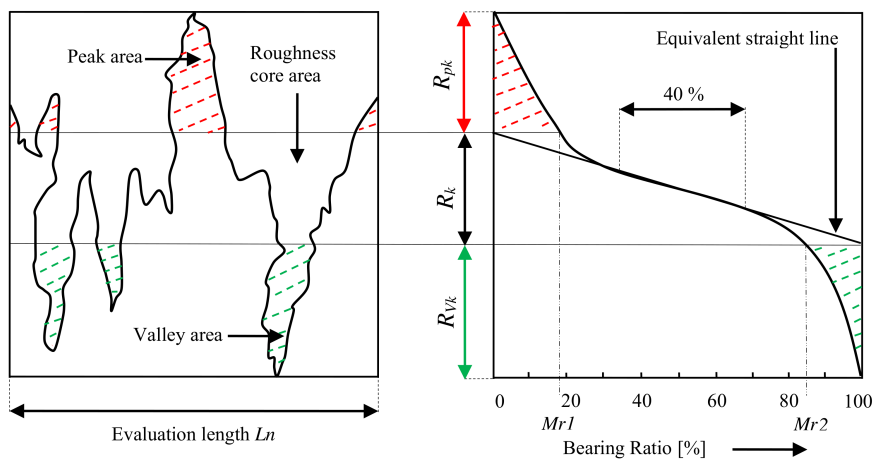


Fig. 2. Bearing area curve (Abbott-Firestone curve)

### 2.3. Planning of experiments

To reduce the number of tests compared to full factorial design (FFD), the experiment was based on Taguchi  $L_{25}$  orthogonal array (25 trials). This method for optimizing cutting parameters offers, compared to others, the advantages of efficiency, simplicity and methodology [25]. Moreover, the Taguchi method is increasingly utilized in machining research [26]. For our study, a factorial plan of three factors was selected with five levels for each. The levels shown in Table 2 were selected in the intervals recommended by the cutting tools manufacturer.

Table 2.

Cutting conditions and their levels

Level	$V_c$ [m/min]	$f$ [mm/rev]	$ap$ [mm]
1	24	0.050	0.10
2	34	0.106	0.15
3	48	0.142	0.20
4	68	0.198	0.25
5	96	0.256	0.30

The diagram in Fig. 3 represents the three input factors and the three measured responses (outputs).

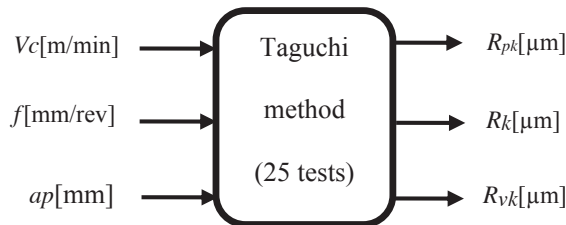


Fig. 3. Input/output parameters

RSM is widely used in science and technology, especially when several input variables influence the results. This analysis technique has been successfully applied to response prediction, design optimization and model validation [27]. The relationship between the cutting conditions (INPUT) and response variations (OUTPUT) is given as follows:

$$Y = F(V_c, f, ap), \quad (1)$$

where  $F$  is the response function and  $Y$  is the corresponding response ( $R_{pk}$ ,  $R_k$  and  $R_{vk}$ ).

In this work, the second-order mathematical model based on the polynomial regression is selected:

$$Y = a_0 + \sum_{i=1}^k a_i X_i + \sum_{ij}^k a_{ij} X_i X_j + \sum_{i=1}^k a_{ii} X_i^2, \quad (2)$$

where  $a_0$  is the free term of the regression equation, the coefficients  $a_1, a_2, \dots, a_k$  and  $a_{11}, a_{22}, a_{kk}$  are the linear and the quadratic terms, respectively. While  $a_{12}, a_{13}, a_{k-1}$  are the interacting terms.  $X_i$  is the input parameters ( $Vc, f$  and  $ap$ ).

### 3. Experimental results and discussion

#### 3.1. Output data table and theirs S/N ratios

The analysis of the impact of cutting conditions ( $Vc, f$  and  $ap$ ) on experimental results and their S/N ratios are given in Table 3.

#### 3.2. ANOVA analysis

Analysis of variance (ANOVA) of experimental results is useful for determining the influence of control factors and their interactions (machining conditions:  $Vc, f$  and  $ap$ ) on the response variation ( $R_{pk}, R_k$  and  $R_{vk}$ ). A factor or interaction can be significant or not when the probability  $p$  value is [28]:

- if  $p$  value  $< 0.05$ , the parameter is significant,
- if  $p$  value  $> 0.05$ , the parameter is insignificant.

The equation of the sum of ( $SS_f$ ) squares is:

$$SS_f = \frac{N}{N_{nf}} \sum_{i=1}^{N_{nf}} (\bar{y}_i - \bar{y})^2, \quad (3)$$

where  $N$  is the total number of experiments,  $N_{nf}$  is the level of each factor  $f$ ,  $\bar{y}_i$  is the average response observed in experiments where factor  $f$  takes its  $i^{\text{th}}$  level and  $\bar{y} = 1/N \sum_{i=1}^N y_i$  is the average of responses.

Mean squares are estimated by following equation:

$$Ms_i = \frac{SS_i}{df_i}. \quad (4)$$

The index  $F$ -ratio is given by following equation:

$$F_i = \frac{Ms_i}{Ms_e}. \quad (5)$$

$Ms_e$  are the mean squares of error.

Table 3.

Experimental results of three output parameters ( $R_{pk}$ ,  $R_k$  and  $R_{vk}$ ) and their  $S/N$  ratios

Trail no.	A: $V_c$	B: $f$	C: $ap$	$R_{pk}$ [ $\mu\text{m}$ ]	$S/N$ [dB]	$R_k$ [ $\mu\text{m}$ ]	$S/N$ [dB]	$R_{vk}$ [ $\mu\text{m}$ ]	$S/N$ [dB]
1	24	0.050	0.10	1.12	-0.98	2.42	-7.67	0.69	-3.22
2	24	0.106	0.15	2.41	-7.64	3.31	-10.39	1.28	2.14
3	24	0.142	0.20	2.47	-7.85	3.43	-10.70	1.33	2.47
4	24	0.198	0.25	2.85	-9.09	3.85	-11.70	1.51	3.57
5	24	0.256	0.30	3.06	-9.71	3.95	-11.93	1.60	4.08
6	34	0.050	0.15	1.01	-0.08	2.09	-6.40	0.57	-4.88
7	34	0.106	0.20	1.78	-5.00	2.80	-8.94	0.84	-1.51
8	34	0.142	0.25	2.14	-6.60	3.23	-10.18	1.21	1.65
9	34	0.198	0.30	2.60	-8.29	3.68	-11.31	1.44	3.16
10	34	0.256	0.10	2.55	-8.13	3.57	-11.05	1.42	3.04
11	48	0.050	0.20	0.54	5.35	1.52	-3.63	0.40	-7.95
12	48	0.106	0.25	1.06	-0.50	2.29	-7.19	0.64	-3.87
13	48	0.142	0.30	1.73	-4.76	2.69	-8.59	0.77	-2.27
14	48	0.198	0.10	1.86	-5.39	2.97	-9.45	0.91	-0.81
15	48	0.256	0.15	1.96	-5.84	3.13	-9.91	1.05	0.42
16	68	0.050	0.25	0.45	6.93	1.44	-3.16	0.38	-8.40
17	68	0.106	0.30	0.75	2.49	1.68	-4.50	0.43	-7.33
18	68	0.142	0.10	1.00	0.00	1.94	-5.75	0.55	-5.19
19	68	0.198	0.15	1.06	-0.50	2.26	-7.08	0.62	-4.15
20	68	0.256	0.20	1.16	-1.28	2.54	-8.09	0.78	-2.15
21	96	0.050	0.30	0.43	7.3	1.36	-2.67	0.36	-8.87
22	96	0.106	0.10	0.26	11.70	1.08	-0.66	0.31	-10.17
23	96	0.142	0.15	0.32	9.89	1.18	-1.43	0.35	-9.11
24	96	0.198	0.20	0.82	1.72	1.78	-5.00	0.48	-6.37
25	96	0.256	0.25	0.96	0.35	1.86	-5.39	0.51	-5.84

The contribution is given by the following equation:

$$Cont.\% = \frac{SS_f}{SS_T} \times 100. \quad (6)$$

The 95% confidence level ( $\alpha = 5\%$ ) is used for the analysis of variance. Tables 4–6 summarize the ANOVA of the experimental results ( $R_{pk}$ ,  $R_k$  and  $R_{vk}$ ).

Table 4 shows that among the significant cutting parameters on the reduced peaks height ( $R_{pk}$ ), the cutting speed is the most significant one with a contribution



of 37.68%, followed by the feed rate with 21.67%, while the depth of cut is the least significant parameter with a percentage of 1.346%. Regarding interactions and products one can clearly see that the two most significant products are:  $V_c \times V_c$  and  $f \times f$  with a contribution of 1.269%, 0.852%, respectively.

Table 4.

ANOVA for  $R_{pk}$  parameter

Source	DF	SS	MS	F value	P value	Cont. %	Remarks
Model	9	17.2982	1.92202	68.41	< 0.0001	97.62	Significant
$V_c$	1	6.6771	6.6771	237.67	< 0.0001	37.68	Significant
$f$	1	3.8398	3.8398	136.68	< 0.0001	21.67	Significant
$ap$	1	0.2385	0.2385	8.49	0.011	1.346	Significant
$V_c \times f$	1	0.0292	0.0292	1.04	0.324	0.165	Insignificant
$V_c \times ap$	1	0.0071	0.0071	0.25	0.622	0.040	Insignificant
$f \times ap$	1	0.0034	0.0034	0.12	0.733	0.019	Insignificant
$V_c^2$	1	0.2250	0.2250	8.01	0.013	1.269	Significant
$f^2$	1	0.1510	0.1510	5.37	0.035	0.852	Significant
$ap^2$	1	0.0021	0.0021	0.08	0.787	0.012	Insignificant
Residual	15	0.4214	0.02809				
Cor total	24	17.7196					

From the analysis of the variance (ANOVA) of the core roughness depth ( $R_k$ ) (Table 5), it can be observed that the three cutting conditions ( $V_c$ ,  $f$  and  $ap$ ) significantly affect the output parameter  $R_k$ . However, the cutting speed ( $V_c$ ) is the most important factor influencing the core roughness depth ( $R_k$ ) with a contribution of 37.65%. The next factor influencing the core roughness depth ( $R_k$ ) is the feed rate ( $f$ ) followed by the depth of cut ( $ap$ ) with contributions of 23.88% and 1.082%, respectively. The product contribution of the feed rate ( $f \times f$ ) is 0.986%. Other terms have a lower contribution to 0.5%.

As shown in Table 6, both speeds ( $V_c$  and  $f$ ) and the product ( $V_c \times V_c$ ) are significant parameters in the reduced valley depth  $R_{vk}$ . The cutting speed was found to be the most significant with a percentage contribution of 36.91%, followed by feed rate (19.50%) and the product of the cutting speed ( $V_c \times V_c$ ) with 1.801%. Other non-significant terms have a contribution of less than 1%. Agrawal et al. [29] concluded through 39 hard turning tests of AISI 4340 (69 HRC), that the feed rate followed by the cutting speed and the cutting depth are the parameters significantly affecting the arithmetic mean roughness  $R_a$ . As reported by Alok et al. [30], ANOVA analysis of the dry hard turning of AISI 52100 steel with a new HSN<sup>2</sup> coated carbide insert indicates that the cutting speed is the first significant

Table 5.

ANOVA for  $R_k$  parameter

Source	<i>DF</i>	<i>SS</i>	<i>MS</i>	<i>F</i> value	<i>P</i> value	<i>Cont. %</i>	Remarks
Model	9	18.2400	2.02666	87.80	< 0.0001	98.14	Significant
$V_c$	1	6.9985	6.9985	303.21	< 0.0001	37.65	Significant
$f$	1	4.4392	4.4392	192.33	< 0.0001	23.88	Significant
$ap$	1	0.2011	0.2011	8.71	0.010	1.082	Significant
$V_c \times f$	1	0.0590	0.0590	2.56	0.131	0.317	Insignificant
$V_c \times ap$	1	0.0526	0.0526	2.28	0.152	0.283	Insignificant
$f \times ap$	1	0.0047	0.0047	0.20	0.657	0.025	Insignificant
$V_c^2$	1	0.0437	0.0437	1.89	0.189	0.235	Insignificant
$f^2$	1	0.1833	0.1833	7.94	0.013	0.986	Significant
$ap^2$	1	0.0068	0.0068	0.30	0.594	0.036	Insignificant
Residual	15	0.3462	0.02308				
Cor total	24	18.5862					

cutting condition on the cutting force with a contribution of 89.13%, followed by the depth of cut (2.57%) and finally the feed rate (2.28%). This tool (HSN<sup>2</sup>) is costing about one-tenth of CBN tool.

Table 6.

ANOVA for  $R_{vk}$  parameter

Source	<i>DF</i>	<i>SS</i>	<i>MS</i>	<i>F</i> value	<i>P</i> value	<i>Cont. %</i>	Remarks
Model	9	4.04834	0.44982	55.87	< 0.0001	97.10	Significant
$V_c$	1	1.5387	1.5387	191.14	< 0.0001	36.91	Significant
$f$	1	0.8130	0.8130	100.99	< 0.0001	19.50	Significant
$ap$	1	0.0243	0.0243	3.02	0.103	0.583	Insignificant
$V_c \times f$	1	0.0142	0.0142	1.76	0.204	0.340	Insignificant
$V_c \times ap$	1	0.0002	0.0002	0.03	0.873	0.004	Insignificant
$f \times ap$	1	0.0010	0.0010	0.13	0.720	0.024	Insignificant
$V_c^2$	1	0.0751	0.0751	9.34	0.008	1.801	Significant
$f^2$	1	0.0144	0.0144	1.79	0.201	0.345	Insignificant
$ap^2$	1	0.0006	0.0006	0.08	0.787	0.014	Insignificant
Residual	15	0.12076	0.00805				
Cor total	24	4.16910					

### 3.3. Regression analysis

Regression analysis appeared as a technique to study the functional relationship between the dependent variable and the independent variables ( $Vc$ ,  $f$  and  $ap$ ) [31]. Based on experimental results, the quadratic regression is used to determine the relationship between the cutting conditions and the three parameters ( $R_{pk}$ ,  $R_k$  and  $R_{vk}$ ). The coefficient of multiple determinations  $R^2$  measures variation proportion in the data points. If  $R^2$  value is very close to +1 (100%), the equation is considered significant [32].

The model of the reduced peaks height  $R_{pk}$  is given by Eq. (7). The determination coefficient of this model is equal to 97.62%.

$$\begin{aligned}
 R_{pk} = & 1.78980 - 0.0640460Vc + 21.2196f - 0.732955ap \\
 & + 0.000340937Vc^2 - 0.0622210Vc \times f + 0.0310595Vc \times ap \\
 & - 32.4492f^2 - 8.50436f \times ap + 4.09748ap^2 \\
 & (R^2 = 97.62\%).
 \end{aligned} \tag{7}$$

The quadratic regression equation of core roughness depth  $R_k$  is given by Eq. (8). The determination coefficient value is 98.14%.

$$\begin{aligned}
 R_k = & 2.76157 - 0.0484485Vc + 20.5352f - 2.30906ap \\
 & + 0.000150177Vc^2 - 0.0884360Vc \times f + 0.0844375Vc \times ap \\
 & - 35.7491f^2 + 10.0335f \times ap - 7.35965ap^2 \\
 & (R^2 = 98.14\%).
 \end{aligned} \tag{8}$$

The quadratic equation of reduced valley depth  $R_{vk}$  is given by Eq. (9). The determination coefficient of this model is equal to 97.10%.

$$\begin{aligned}
 R_{vk} = & 0.836586 - 0.0307799Vc + 9.32216f + 1.75402ap \\
 & + 0.000197061Vc^2 - 0.0433723Vc \times f + 0.00537516Vc \times ap \\
 & - 10.0318f^2 - 4.77682f \times ap - 2.19134ap^2 \\
 & (R^2 = 97.10\%).
 \end{aligned} \tag{9}$$

The previous three models of the components of the BAC can be used to predict surface roughness. Fig. 4 shows a comparison between predicted and measured values of the bearing ratio curve components. The results of this study confirm that the actual values are very close to the predicted values. In addition, the three non-linear models are statistically significant with ( $P < 0.05$ ), and hence the validity of the models can be confirmed. These quadratic models could probably contribute to predicting the values of bearing ratio curve parameters in the range of cutting conditions used.

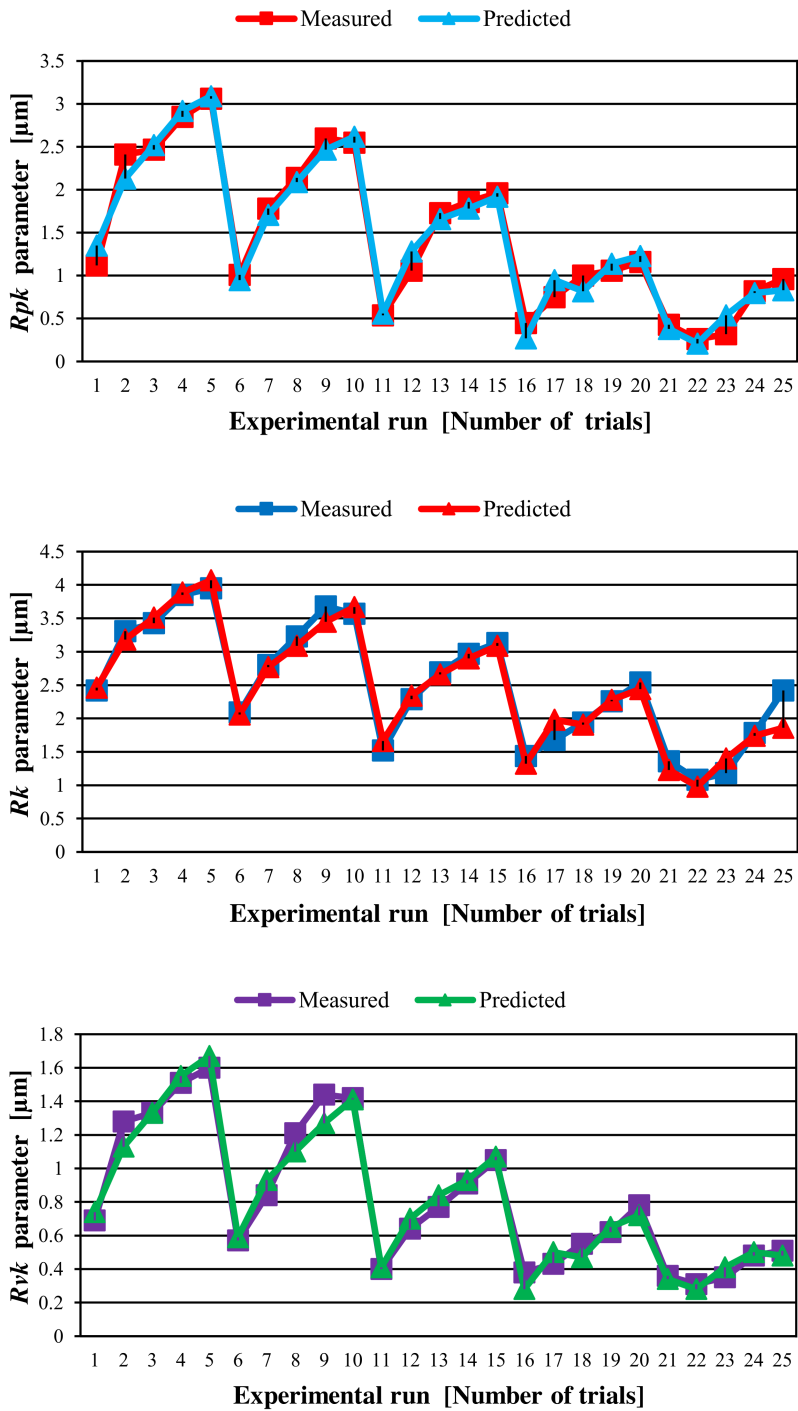


Fig. 4. Comparison between measured and predicted values for the bearing curve components

### 3.4. Response surface analysis

Fig. 5 shows in 3D response surfaces of three dependent variables ( $R_{pk}$ ,  $R_k$  and  $R_{vk}$ ) under the effect of interactions of three process variables ( $Vc$ ,  $f$  and  $ap$ ). So, the possible interactions are:  $Vc \times f$ ,  $Vc \times ap$  and  $ap \times f$ . In the figure and for each interaction, the not shown control factor is kept constant for the intermediate level ( $Vc = 48$  m/min,  $f = 0.142$  mm/rev,  $ap = 0.20$  mm). As shown in this Fig. 5

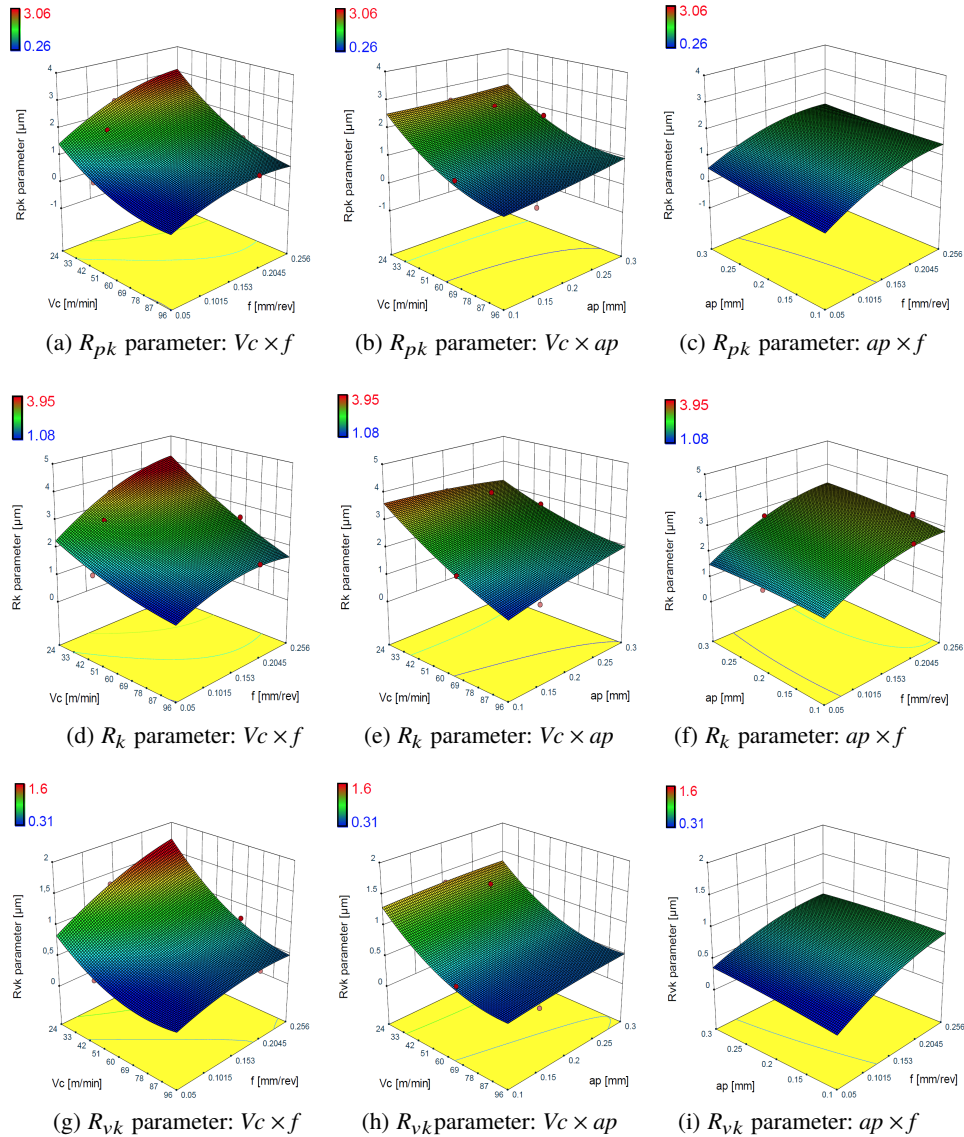


Fig. 5. 3D response surface obtained for different interactions: left:  $R_{pk}$  parameter, middle:  $R_k$  parameter, right:  $R_{vk}$  parameter

(a, b, d, and g), the slope of cutting speed is greater relative to slope of the two other factors, there by implying that it is the first cutting condition affecting the output parameters. The second significant parameter is the feed rate ( $f$ ) followed by the depth of cut ( $ap$ ). Furthermore, the interaction ( $Vc \times f$ ) appears as a significant term for the parameters of Abbott-Firestone curve. These results are in agreement with the work of Alok and Das [33] who found that the cutting speed is the most important parameter influencing the arithmetic mean roughness  $Ra$ . According to response surface methodology (RSM) performed by Hessainia et al. [34] during hard turning of AISI 4140 steel (56 HRC), the feed rate and the depth of cut are the two cutting conditions most affecting arithmetic average roughness  $Ra$ .

### 3.5. Optimization

#### 3.5.1. Mono-objective optimization using S/N ratio

In order to analyze the experimental results, the signal-to-noise ratio ( $S/N$ ) is used because it is the core criterion in the Taguchi method [35]. The signal-to-noise ratio ( $S/N$ ) optimizes the control factors [36]. These are the variables that can be controlled in a practical and economical way [37]. The purpose of this study is to minimize  $R_{pk}$  and  $R_k$  parameters while maximizing  $R_{vk}$  parameter to improve the quality of bearing area curve (BAC). According to this method, to obtain optimal cutting conditions, the  $S/N$  ratio must have a maximum value for the three parameters ( $R_{pk}$ ,  $R_k$  and  $R_{vk}$ ). The  $S/N$  ratio is generally divided into three categories given by the following equations [38, 39]:

Nominal is the best:

$$S/N = 10 \log \left( \frac{\bar{y}}{s_y^2} \right). \quad (10)$$

The-smaller-is-the better:

$$S/N = -10 \log \left( \frac{1}{n} \sum_{i=1}^n y_i^2 \right). \quad (11)$$

The-larger-is-the better:

$$S/N = -10 \log \left( \frac{1}{n} \sum_{i=1}^n \frac{1}{y_i^2} \right). \quad (12)$$

The  $S/N$  ratio of both  $R_{pk}$  and  $R_k$  parameters is calculated using Eq. (11) “The smaller is the better (minimize)”. On the other hand, the reduced valley depth  $R_{vk}$  was calculated using Eq. (12) “The-larger is the better (maximize)”. The experimental results of the parameters of Abbott-Firestone curve and their signal-to-noise ( $S/N$ ) ratios are shown in Table 3.

By Taguchi design, Table 7 shows the optimal levels of cutting conditions for the optimal values of three parameters of the material ratio curve. These values are graphically represented (Figs. 6–8). From these graphs and Table 7, one can see that optimal cutting conditions are easily determined to minimize the first two BAC parameters and maximize the last one. The best levels correspond to higher  $S/N$  ratio values of the three parameters ( $R_{pk}$ ,  $R_k$  and  $R_{vk}$ ). So, the levels and  $S/N$  ratios of the three factors (A:  $V_c$ , B:  $f$  and C:  $ap$ ) giving the best values of three parameters ( $R_{pk}$ ,  $R_k$  and  $R_{vk}$ ) are: for  $R_{pk}$  (factor A (level 5,  $S/N = 6.201$ ),

Table 7.

$S/N$  response table for (a)  $R_{pk}$  parameter, (b)  $R_k$  parameter, and (c)  $R_{vk}$  parameter;  
(a) and (b): the-smaller-is-the better, (c) the-larger-is-the better

Trail no	A: $V_c$ [m/min]	B: $f$ [mm/rev]	C: $ap$ [mm]
----------	------------------	-----------------	--------------

(a)

1	-7.058	<b>3.709</b>	<b>-0.561</b>
2	-5.626	0.208	-0.836
3	-2.230	-1.865	-1.415
4	1.527	-4.313	-1.784
5	<b>6.201</b>	-4.925	-2.589
Delta	13.259	8.634	2.028
Rank	1	2	3

(b)

1	-10.484	<b>-4.711</b>	<b>-6.922</b>
2	-9.580	-6.342	-7.046
3	-7.759	-7.336	-7.278
4	-5.722	-8.914	-7.529
5	<b>-3.035</b>	-9.277	-7.804
Delta	7.449	4.566	0.882
Rank	1	2	3

(c)

1	<b>1.812</b>	-6.668	-3.272
2	0.294	-4.150	-3.117
3	-2.900	-2.489	-3.105
4	-5.447	-0.919	-2.578
5	-8.077	<b>-0.090</b>	<b>-2.245</b>
Delta	9.889	6.577	1.027
Rank	1	2	3

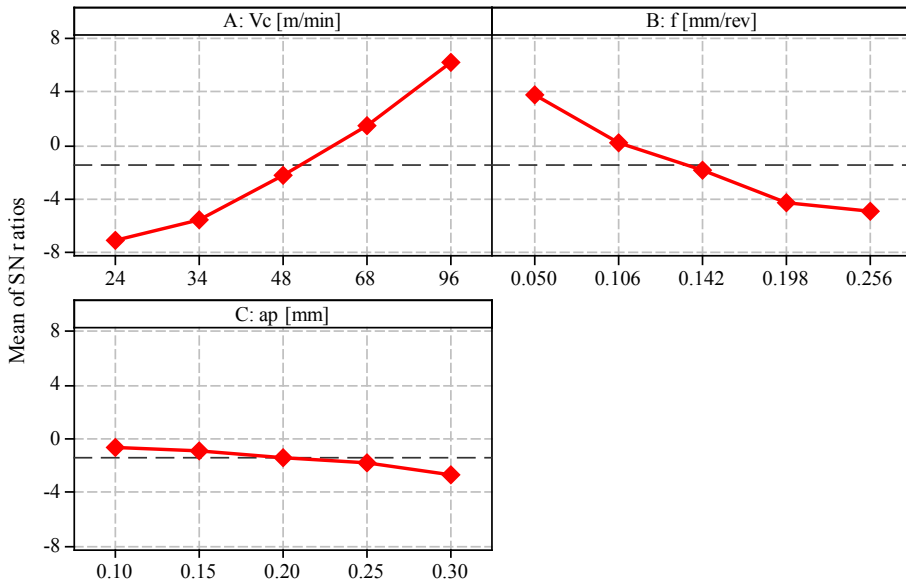


Fig. 6. Impact of cutting conditions on  $S/N$  ratio for  $R_{pk}$  parameter

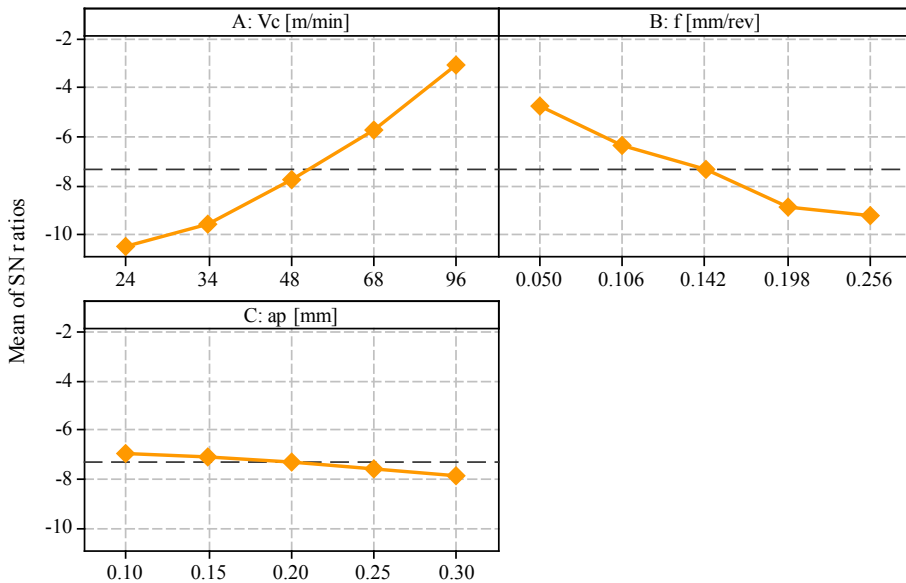


Fig. 7. Impact of cutting conditions on  $S/N$  ratio for  $R_k$  parameter

factor B (level 1,  $S/N = 3.709$ ) and factor C (level 1,  $S/N = -0.561$ ), for  $R_k$  (factor A (level 5,  $S/N = -3.035$ ), factor B (level 1,  $S/N = -4.711$ ) and factor C (level 1,  $S/N = -6.922$ )), and for  $R_{vk}$  (factor A (level 1,  $S/N = 1.812$ ), factor B (level 5,  $S/N = -0.090$ ) and factor C (level 5,  $S/N = -2.245$ )). Indeed, we can



see that the slope of the cutting speed ( $V_c$ ) is greater than the slope of the feed rate and the depth of cut (lower slope) (Figs. 6–8). These figures show that the cutting speed has the most significant effect whereas the depth of cut has the least significant one. In this context, the optimal values for  $R_{pk}$ ,  $R_k$  and  $R_{vk}$  parameters of the bearing ratio curve are obtained for a cutting speed of 96 m/min (A5), a feed rate of 0.106 mm/rev (B2) and a depth of cut 0.10 mm (C1) because the value of  $R_{vk} = 0.31 \mu\text{m}$  is a large value for supplying, circulating and storing the oil during engine running. As a matter of comparison, Meddour et al. [23] found that both  $S_k$  and  $S_{pk}$  surface parameters decrease with increasing cutting speed when turning AISI 4140 steel hardened to 60 HRC. Khellouki et al. [40] showed that if working on AISI 52100 bearing steel hardened to 62 HRC, the core roughness depth  $R_k$  drops from 0.9  $\mu\text{m}$  for hard turning to 0.38  $\mu\text{m}$  for belt finishing.

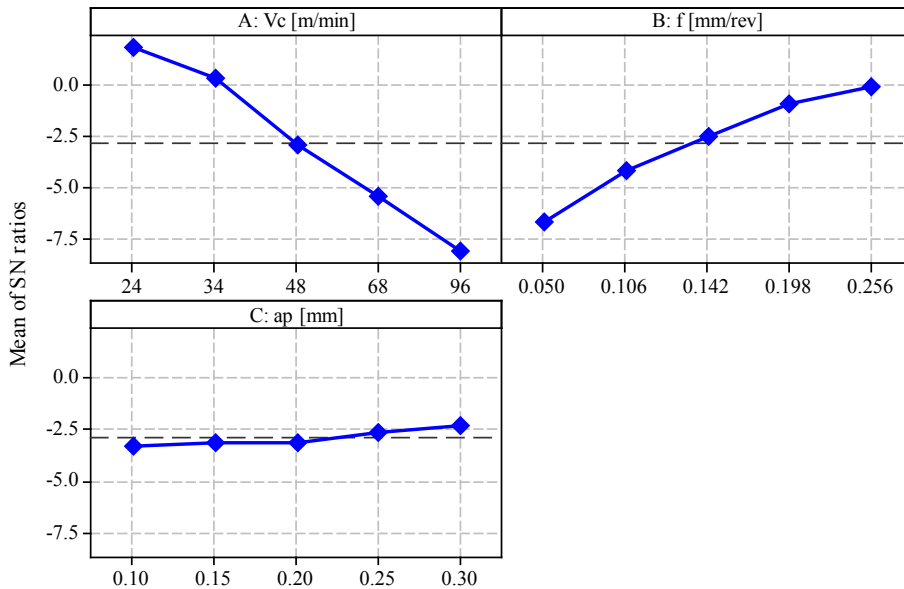


Fig. 8. Impact of cutting conditions on  $S/N$  ratio for  $R_{vk}$  parameter

### 3.5.2. Multi-objective optimization using DF

In this section, the main purpose of digital optimization is to find the optimum values of the machining conditions of 16MC5 hard turning steel to produce the lowest value of the bearing ratio curve parameters ( $R_{pk}$  and  $R_k$ ) and the highest value of the other parameter ( $R_{vk}$ ). The desirability function (DF) is employed to optimize the output parameters. The goal of cutting conditions and the response parameters, and their upper and lower limits are illustrated in Table 8. Tables 9–11 summarize the results of optimizing response parameters, using RSM, of the material ratio curve  $R_{pk}$ ,  $R_k$  and  $R_{vk}$ , respectively. The contour graph is shown in Fig. 9.

Table 8.

## Conditions for optimization of hard turning parameters

Conditions	Goal	Lower limit	Upper limit
Cutting speed, $V_c$ [m/min]	In range	24	96
Feed rate, $f$ [mm/rev]	In range	0.050	0.256
Depth of cut, $ap$ [mm]	In range	0.10	0.30
$R_{pk}$ parameter, [ $\mu\text{m}$ ]	Minimize	0.26	3.06
$R_k$ parameter, [ $\mu\text{m}$ ]	Minimize	1.08	3.95
$R_{vk}$ parameter, [ $\mu\text{m}$ ]	Maximize	0.31	1.6

Table 9.

Response optimization for  $R_{pk}$  parameter

Solution no.	$V_c$ [m/min]	$f$ [mm/rev]	$ap$ [mm]	$R_{pk}$ [ $\mu\text{m}$ ]	Desirability	Remarks
1	95.262	0.053	0.108	0.245	1.000	Selected
2	81.177	0.254	0.100	0.252	1.000	
3	89.042	0.256	0.101	0.117	1.000	
4	95.554	0.252	0.104	0.073	1.000	

Table 10.

Response optimization for  $R_k$  parameter

Solution no.	$V_c$ [m/min]	$f$ [mm/rev]	$ap$ [mm]	$R_k$ [ $\mu\text{m}$ ]	Desirability	Remarks
1	96.000	0.050	0.100	0.479	0.953	Selected
2	96.000	0.050	0.101	0.492	0.950	
3	95.726	0.050	0.100	0.493	0.950	
4	95.936	0.051	0.100	0.501	0.948	

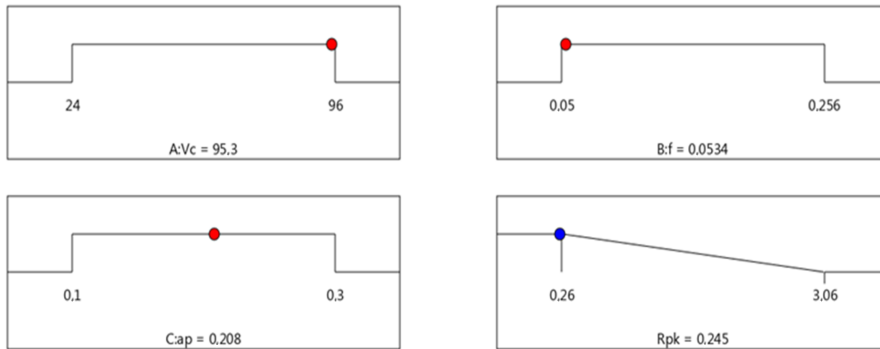
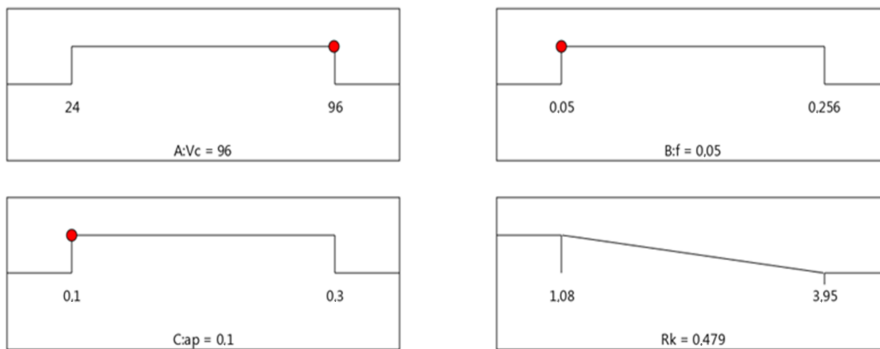
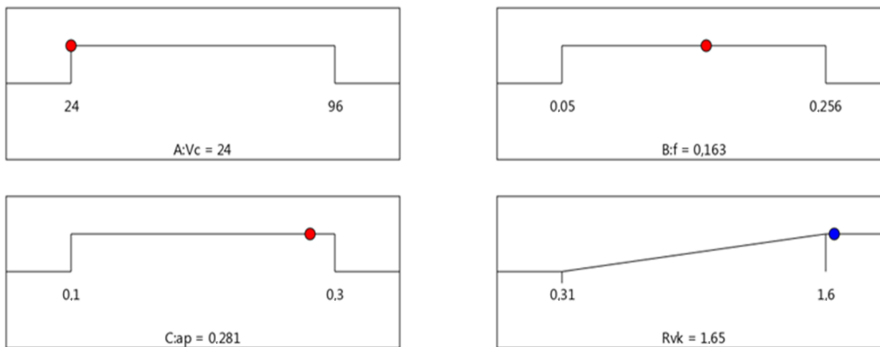
Table 11.

Response optimization for  $R_{vk}$  parameter

Solution no.	$V_c$ [m/min]	$f$ [mm/rev]	$ap$ [mm]	$R_{vk}$ [ $\mu\text{m}$ ]	Desirability	Remarks
1	24.000	0.163	0.281	1.646	0.892	Selected
2	24.000	0.163	0.282	1.646	0.892	
3	24.000	0.163	0.282	1.646	0.892	
4	24.000	0.162	0.282	1.645	0.892	

From Tables 9–11 and Fig. 9, the values of the optimal cutting parameters to achieve a better quality of the bearing area curve (BAC) are:

- $R_{pk} = 0.24 \mu\text{m}$ :  $V_c = 95 \text{ m/min}$ ,  $f = 0.05 \text{ mm/rev}$  and  $ap = 0.2 \text{ mm}$ ,
- $R_k = 0.47 \mu\text{m}$ :  $V_c = 96 \text{ m/min}$ ,  $f = 0.05 \text{ mm/rev}$  and  $ap = 0.1 \text{ mm}$ ,
- $R_{vk} = 1.65 \mu\text{m}$ :  $V_c = 24 \text{ m/min}$ ,  $f = 0.16 \text{ mm/rev}$  and  $ap = 0.28 \text{ mm}$ .

(a)  $R_{pk}$  parameter: desirability = 1.000(b)  $R_k$  parameter: desirability = 0.953(c)  $R_{vk}$  parameter: desirability = 0.892Fig. 9. Desirability function graph for output parameters ( $R_{pk}$ ,  $R_k$  and  $R_{vk}$ )

So, the optimal cutting regime chosen is:  $V_c = 96$  m/min,  $f = 0.05$  mm/rev and  $ap = 0.1$  mm, since the value of reduced valley depth  $R_{vk} = 0.31 \mu\text{m}$  is a large value for oil supply, circulation and storage during engine operation.

## 4. Conclusions

The objective of this work was to study the impact of technological parameters (cutting speed ( $V_c$ ), feed rate ( $f$ ) and depth of cut ( $ap$ )) during hard turning operation of 16MC5 steel on the Abbott-Firestone curve components (the roughness peaks ( $R_{pk}$ ), the roughness core ( $R_k$ ) and the valleys ( $R_{vk}$ )) and finding the role of each machining parameter. The main conclusions drawn from this study are:

- The  $S/N$  report shows that the cutting speed ( $V_c$ ) is the most fundamental factor affecting the bearing area curve components ( $R_{pk}$ ,  $R_k$  and  $R_{vk}$ ) whereas the depth of cut ( $ap$ ) is the least significant.
- The statistical analysis of variance (ANOVA) confirmed that the cutting speed ( $V_c$ ) has the strongest effect on the three criteria of Abbott curve, followed by feed rate ( $f$ ). While the depth of cut ( $ap$ ) is the third significant cutting parameter on the first two parameters ( $R_{pk}$  and  $R_k$ ) and not significant on the reduced valley depth ( $R_{vk}$ ). The percentage contribution of the cutting speed ( $V_c$ ) are (37.68%, 37.65%, 36.91%), on the output parameters  $R_{pk}$ ,  $R_k$  and  $R_{vk}$ , respectively.
- Comparison of the experimental and estimated results clearly shows that the models resulting from the quadratic regression method give satisfactory results ( $R^2(R_{pk}) = 97.62\%$ ,  $R^2(R_k) = 98.14\%$  and  $R^2(R_{vk}) = 97.1\%$ ). A good agreement has been reached between the two results.
- The mathematical models found represent a considerable interest in mechanics and industry, since they help making predictions.
- The hard machining parameters obtained by the desirability function (DF) method are: cutting speed (96 m/min), feed rate (0.05 mm/rev) and depth of cut (0.1 mm), since the value of  $R_{vk} = 0.31 \mu\text{m}$  is a great value to supply, circulate and store oil during engine operation, so the engine runs long.
- Under these working conditions, the bearing area curve is improved and this makes it possible to: reduce running-in time, wear rate and oil consumption (the curve is relatively a horizontal line in its intermediate part). Thus, the turned surface approaches the configuration which characterizes a 'plateau' surface. This kind of surface is required for its good bearing properties.

Manuscript received by Editorial Board, December 15, 2019;  
final version, March 14, 2020.

## References

- [1] W. Grzesik and K. Żak. Modification of surface finish produced by hard turning using superfinishing and burnishing operations. *Journal of Materials Processing Technology*, 212(1):315–322, 2012. doi: [10.1016/j.jmatprotec.2011.09.017](https://doi.org/10.1016/j.jmatprotec.2011.09.017).
- [2] W. Grzesik and T. Wanat. Comparative assessment of surface roughness produced by hard machining with mixed ceramic tools including 2D and 3D analysis. *Journal of Materials Processing Technology*, 169(3):364–371, 2005. doi: [10.1016/j.jmatprotec.2005.04.080](https://doi.org/10.1016/j.jmatprotec.2005.04.080).

- [3] B. Fnides, H. Aouici, M. Elbah, S. Boutabba, and L. Boulanouar. Comparison between mixed ceramic and reinforced ceramic tools in terms of cutting force components modelling and optimization when machining hardened steel AISI 4140 (60 HRC). *Mechanics & Industry*, 16(6):609, 2015. doi: [10.1051/meca/2015036](https://doi.org/10.1051/meca/2015036).
- [4] H. Aouici, H. Bouchelaghem, M.A. Yallese, M. Elbah, and B. Fnides. Machinability investigation in hard turning of AISI D3 cold work steel with ceramic tool using response surface methodology. *The International Journal of Advanced Manufacturing Technology*, 73(9-12):1775–1788, 2014. doi: [10.1007/s00170-014-5950-0](https://doi.org/10.1007/s00170-014-5950-0).
- [5] M. Dogra, V.S. Sharma, A. Sachdeva, N.M. Suri, and J.S. Dureja. Tool wear, chip formation and workpiece surface issues in CBN hard turning: A review. *International Journal of Precision Engineering and Manufacturing*, 11(2):341–358, 2010. doi: [10.1007/s12541-010-0040-1](https://doi.org/10.1007/s12541-010-0040-1).
- [6] V. Bhemuni, S.R. Chalamalasetti, P.K. Konchada, and V.V. Pragada. Analysis of hard turning process: thermal aspects. *Advances in Manufacturing*, 3(4):323–330, 2015. doi: [10.1007/s40436-015-0124-3](https://doi.org/10.1007/s40436-015-0124-3).
- [7] F. Klocke, E. Brinksmeier, and K. Weinert. Capability profile of hard cutting and grinding processes. *CIRP Annals*, 54(2):22–45, 2005. doi: [10.1016/S0007-8506\(07\)60018-3](https://doi.org/10.1016/S0007-8506(07)60018-3).
- [8] A. Khellouki, J. Rech, and H. Zahouani. The effect of lubrication conditions on belt finishing. *International Journal of Machine Tools and Manufacture*, 50(10):917–921, 2010. doi: [10.1016/j.ijmactools.2010.04.004](https://doi.org/10.1016/j.ijmactools.2010.04.004).
- [9] K. Mondal, S. Das, B. Mandal, and D. Sarkar. An investigation on turning hardened steel using different tool inserts. *Materials and Manufacturing Processes*, 31(13):1770–1781, 2016. doi: [10.1080/10426914.2015.1117634](https://doi.org/10.1080/10426914.2015.1117634).
- [10] C. Duan, F. Zhang, W. Sun, X. Xu, and M. Wang. White layer formation mechanism in dry turning hardened steel. *Journal of Advanced Mechanical Design, Systems, and Manufacturing*, 12(2):1–12, 2018. doi: [10.1299/jamdsm.2018jamdsm0044](https://doi.org/10.1299/jamdsm.2018jamdsm0044).
- [11] P. Revel, N. Jouini, G. Thoquenne, and F. Lefebvre. High precision hard turning of AISI 52100 bearing steel. *Precision Engineering*, 43:24–34, 2016. doi: [10.1016/j.precisioneng.2015.06.006](https://doi.org/10.1016/j.precisioneng.2015.06.006).
- [12] S. Saini, I. Singh Ahuja, and V.S. Sharma. Influence of cutting parameters on tool wear and surface roughness in hard turning of AISI H11 tool steel using ceramic tools. *International Journal of Precision Engineering and Manufacturing*, 13(8):1295–1302, 2012. doi: [10.1007/s12541-012-0172-6](https://doi.org/10.1007/s12541-012-0172-6).
- [13] D. Manivel and R. Gandhinathan. Optimization of surface roughness and tool wear in hard turning of austempered ductile iron (grade 3) using Taguchi method. *Measurement*, 93:108–116, 2016. doi: [10.1016/j.measurement.2016.06.055](https://doi.org/10.1016/j.measurement.2016.06.055).
- [14] G. Bartarya and S.K. Choudhury. Effect of cutting parameters on cutting force and surface roughness during finish hard turning AISI52100 grade steel. *Procedia CIRP*, 1:651–656, 2012. doi: [10.1016/j.procir.2012.05.016](https://doi.org/10.1016/j.procir.2012.05.016).
- [15] H. Aouici, M.A. Yallese, K. Chaoui, T. Mabrouki, and J.F. Rigal. Analysis of surface roughness and cutting force components in hard turning with CBN tool: Prediction model and cutting conditions optimization. *Measurement*, 45(3):344–353, 2012. doi: [10.1016/j.measurement.2011.11.011](https://doi.org/10.1016/j.measurement.2011.11.011).
- [16] M.W. Azizi, S. Belhadi, M.A. Yallese, T. Mabrouki, and J.F. Rigal. Surface roughness and cutting forces modeling for optimization of machining condition in finish hard turning of AISI 52100 steel. *Journal of Mechanical Science and Technology*, 26(12):4105–4114, 2012. doi: [10.1007/s12206-012-0885-6](https://doi.org/10.1007/s12206-012-0885-6).
- [17] S.K. Shihab, Z.A. Khan, A.N. Siddiquee, and N.Z. Khan. A novel approach to enhance performance of multilayer coated carbide insert in hard turning. *Archive of Mechanical Engineering*, 62(4):539–552, 2015. doi: [10.1515/meceng-2015-0030](https://doi.org/10.1515/meceng-2015-0030).

- [18] N. Jouini, P. Revel, P.E. Mazeran, and M. Bigerelle. The ability of precision hard turning to increase rolling contact fatigue life. *Tribology International*, 59:141–146, 2013. doi: [10.1016/j.triboint.2012.07.010](https://doi.org/10.1016/j.triboint.2012.07.010).
- [19] N. Jouini, P. Revel, G. Thoquenne, and F. Lefebvre. Characterization of surfaces obtained by precision hard turning of AISI 52100 in relation to RCF life. *Procedia Engineering*, 66:793–802, 2013. doi: [10.1016/j.proeng.2013.12.133](https://doi.org/10.1016/j.proeng.2013.12.133).
- [20] N. Jouini, P. Revel, and M. Bigerelle. Relevance of roughness parameters of surface finish in precision hard turning. *Scanning*, 36(1):86–94, 2014. doi: [10.1002/sca.21100](https://doi.org/10.1002/sca.21100).
- [21] G. Rotella, D. Umbrello, O.W. Dillon Jr., and I.S. Jawahir. Evaluation of process performance for sustainable hard machining. *Journal of Advanced Mechanical Design, Systems, and Manufacturing*, 6(6):989–998, 2012. doi: [10.1299/jamdsm.6.989](https://doi.org/10.1299/jamdsm.6.989).
- [22] I. Meddour, M.A. Yallese, R. Khattabi, M. Elbah, and L. Boulanouar. Investigation and modeling of cutting forces and surface roughness when hard turning of AISI 52100 steel with mixed ceramic tool: cutting conditions optimization. *The International Journal of Advanced Manufacturing Technology*, 77(5-8):1387–1399, 2014. doi: [10.1007/s00170-014-6559-z](https://doi.org/10.1007/s00170-014-6559-z).
- [23] I. Meddour, M.A. Yallese, H. Bensouilah, A. Khellaf, and M. Elbah. Prediction of surface roughness and cutting forces using RSM, ANN, and NSGA-II in finish turning of AISI 4140 hardened steel with mixed ceramic tool. *The International Journal of Advanced Manufacturing Technology*, 97(5-8):1931–1949, 2018. doi: [10.1007/s00170-018-2026-6](https://doi.org/10.1007/s00170-018-2026-6).
- [24] S. Siraj, H.M. Dharmadhikari, and N. Gore. Modeling of roughness value from tribological parameters in hard turning of AISI 52100 steel. *Procedia Manufacturing*, 20:344–349, 2018. doi: [10.1016/j.promfg.2018.02.050](https://doi.org/10.1016/j.promfg.2018.02.050).
- [25] H. Bensouilah, H. Aouici, I. Meddour, M.A. Yallese, T. Mabrouki, and F. Girardin. Performance of coated and uncoated mixed ceramic tools in hard turning process. *Measurement*, 82:1–18, 2016. doi: [10.1016/j.measurement.2015.11.042](https://doi.org/10.1016/j.measurement.2015.11.042).
- [26] E. Yücel and M. Günay. Modelling and optimization of the cutting conditions in hard turning of high-alloy white cast iron (Ni-Hard). *Proceedings of the Institution of Mechanical Engineers, Part C: Journal of Mechanical Engineering Science*, 227(10):2280–2290, 2012. doi: [10.1177/0954406212471755](https://doi.org/10.1177/0954406212471755).
- [27] M. Elbah, H. Aouici, I. Meddour, M.A. Yallese, and L. Boulanouar. Application of response surface methodology in describing the performance of mixed ceramic tool when turning AISI 4140 steel. *Mechanics & Industry*, 17(3):309, 2016. doi: [10.1051/meca/2015076](https://doi.org/10.1051/meca/2015076).
- [28] L. Bouzid, M.A. Yallese, K. Chaoui, T. Mabrouki, and L. Boulanouar. Mathematical modeling for turning on AISI 420 stainless steel using surface response methodology. *Proceedings of the Institution of Mechanical Engineers, Part B: Journal of Engineering Manufacture*, 229(1):45–61, 2014. doi: [10.1177/0954405414526385](https://doi.org/10.1177/0954405414526385).
- [29] A. Agrawal, S. Goelb, W. Bin Rashid, and M. Pric. Prediction of surface roughness during hard turning of AISI 4340 steel (69 HRC). *Applied Soft Computing*, 30:279–286, 2015. doi: [10.1016/j.asoc.2015.01.059](https://doi.org/10.1016/j.asoc.2015.01.059).
- [30] A. Alok and M. Das. Multi-objective optimization of cutting parameters during sustainable dry hard turning of AISI 52100 steel with newly develop HSN<sup>2</sup>-coated carbide insert. *Measurement*, 133:288–302, 2019. doi: [10.1016/j.measurement.2018.10.009](https://doi.org/10.1016/j.measurement.2018.10.009).
- [31] O. Zerti, M.A. Yallese, R. Khettabi, K. Chaoui, and T. Mabrouki. Design optimization for minimum technological parameters when dry turning of AISI D3 steel using Taguchi method. *The International Journal of Advanced Manufacturing Technology*, 89(5-8):1915–1934, 2017. doi: [10.1007/s00170-016-9162-7](https://doi.org/10.1007/s00170-016-9162-7).
- [32] S. Chinchankar and S.K. Choudhury. Effect of work material hardness and cutting parameters on performance of coated carbide tool when turning hardened steel: An optimization approach. *Measurement*, 46(4):1572–1584, 2013. doi: [10.1016/j.measurement.2012.11.032](https://doi.org/10.1016/j.measurement.2012.11.032).

- [33] A. Alok and M. Das. Cost effective way of hard turning with newly developed HSN2 coated tool. *Materials and Manufacturing Processes*, 33(9):1003–1010, 2018. doi: [10.1080/10426914.2017.1388521](https://doi.org/10.1080/10426914.2017.1388521).
- [34] Z. Hessainia, M.A. Yallese, L. Bouzid, and T. Mabrouki. On the application of response surface methodology for predicting and optimizing surface roughness and cutting forces in hard turning by PVD coated insert. *International Journal of Industrial Engineering Computations*, 6(2):267–284, 2015. doi: [10.5267/j.ijiec.2014.10.003](https://doi.org/10.5267/j.ijiec.2014.10.003).
- [35] İ. Asiltürk and H. Akkuş. Determining the effect of cutting parameters on surface roughness in hard turning using the Taguchi method. *Measurement*, 44(9):1697–1704, 2011. doi: [10.1016/j.measurement.2011.07.003](https://doi.org/10.1016/j.measurement.2011.07.003).
- [36] T. Kivak. Optimization of surface roughness and flank wear using the Taguchi method in milling of Hadfield steel with PVD and CVD coated inserts. *Measurement*, 50:19–28, 2014. doi: [10.1016/j.measurement.2013.12.017](https://doi.org/10.1016/j.measurement.2013.12.017).
- [37] T. Kivak, G. Samtaş, and A. Çiçek. Taguchi method based optimization of drilling parameters in drilling of AISI 316 steel with PVD monolayer and multilayer coated HSS drills. *Measurement*, 45(6):1547–1557, 2012. doi: [10.1016/j.measurement.2012.02.022](https://doi.org/10.1016/j.measurement.2012.02.022).
- [38] M. Nalbant, H. Gökaya, and G. Sur. Application of Taguchi method in the optimization of cutting parameters for surface roughness in turning. *Materials & Design*, 28(4):1379–1385, 2007. doi: [10.1016/j.matdes.2006.01.008](https://doi.org/10.1016/j.matdes.2006.01.008).
- [39] R. Shetty, R.B. Pai, S.S. Rao, and R. Nayak. Taguchi’s technique in machining of metal matrix composites. *Journal of the Brazilian Society of Mechanical Sciences and Engineering*, 31(1):12–20, 2009. doi: [10.1590/S1678-58782009000100003](https://doi.org/10.1590/S1678-58782009000100003).
- [40] A. Khellouki, J. Rech, and H. Zahouani. The effect of abrasive grain’s wear and contact conditions on surface texture in belt finishing. *Wear*, 263(1-6):81–87, 2007. doi: [10.1016/j.wear.2006.11.037](https://doi.org/10.1016/j.wear.2006.11.037).